GEOLOGICA CARPATHICA, 55, 4, BRATISLAVA, AUGUST 2004
311–323

PALEOCEANOGRAPHY OF THE WESTERN CENTRAL PARATETHYS DURING EARLY OLIGOCENE NANNOPLANKTON ZONE NP23 IN THE AUSTRIAN MOLASSE BASIN

HANS-MARTIN SCHULZ[1], ACHIM BECHTEL[2*], THOMAS RAINER[2], REINHARD F. SACHSENHOFER[2] and ULRICH STRUCK[3]

[1]Department of Petroleum Geology, Institute of Geology and Paleontology, Technical University of Clausthal, Leibnizstr. 10, D-38678 Clausthal-Zellerfeld, Germany; schulz@geologie.tu-clausthal.de
[2]Department of Geosciences, Montanuniversität Leoben, Peter-Tunner-Str. 5, A-8700 Leoben, Austria
*Present address: Institute of Mineralogy and Petrology, University of Bonn, Poppelsdorfer Schloss, D-53115 Bonn, Germany
[3]GeoBio-Center, Ludwig-Maximilians-University, Richard-Wagner-Str. 10, D-80333 München, Germany

(Manuscript received April 30, 2003; accepted in revised form October 2, 2003)

Abstract: The 5.5 m thick Dynow Marlstone in well Oberschauersberg 1 in the Upper Austrian Molasse Basin was studied using mineral and maceral petrography, SEM, organic geochemistry, and C- and N-isotopy of the organic material. The well is located on the former upper slope of the northern basin margin. The depositional period of the Dynow Marlstone covers parts of the Early Oligocene nannoplankton Zone NP23, which corresponds to the culmination of the first Paratethys isolation. The Dynow Marlstone represents a carbonate-rich, organic-poor interval (0.5–2 % TOC) intercalated between organic-rich formations. The onset of the deposition of the Dynow Marlstone was characterized by an abrupt increase in primary carbonate productivity, but persisting photic zone anoxia. Both high organic carbon productivity and photic zone anoxia prevailed during deposition of the Dynow Marlstone. These constant conditions were overprinted by cyclic increases in the trophic level favouring blooms of calcareous nannoplankton. Limestones with low TOC contents were deposited during algal blooms, whereas organic-rich marls accumulated during periods with low production of calcareous nannoplankton. Sulphate reduction extended into the water column. The intensive consumption of labile organic material decreased the hydrogen index. Intensified photic zone anoxia and an increase in salinity worsened the ecological environment for calcareous nannoplankton and led to deposition of the organic-rich marls of the Eggerding Formation within a constantly eutrophic and normal-marine environment.

Key words: Kiscellian, Paratethys, Dynow Marlstone, paleoceanography, C–N isotopes, biomarker, organic carbon.

Introduction

The separation of the Paratethys from the Tethys commenced at the Eocene/Oligocene boundary and reached a maximum during middle Kiscellian time in the nannoplankton Zone NP23 of Martini 1971 (32.2–30 Ma; Rögl 1996) when the Paratethys lost its connection to the World Ocean (Solenovian Event, e.g. Popov et al. 1993; Fig. 1). Basin isolation was coupled to the development of dysaerobic to anoxic bottom water conditions from the Molasse Basin to the Caspian Sea (Rögl 1999). These favoured the deposition of organic-rich rocks acting as hydrocarbon source rocks in several Paratethyan basins including the Molasse Basin (Wehner & Kuckelkorn 1995; Schmidt & Erdogan 1996; Ziegler & Roure 1999).

Deposition of organic-rich sediments in the western Central Paratethys (e.g. Upper Austrian Molasse Basin) commenced during the latest Priabonian and continued till Early Miocene (Egerian) times, but was progressively focussed to the northern basin slope (Fig. 2). Different paleoceanographic models have been proposed for the formation of the organic-rich rocks. Many authors favour a stagnant basin model for the formation of Kiscellian rocks (Gerhard 1982, 1988; Dohmann 1991; Schulz et al. 2002), whereas Wagner (1996, 1998) considering the asymmetric facies distribution during Egerian times proposed an upwelling scenario.

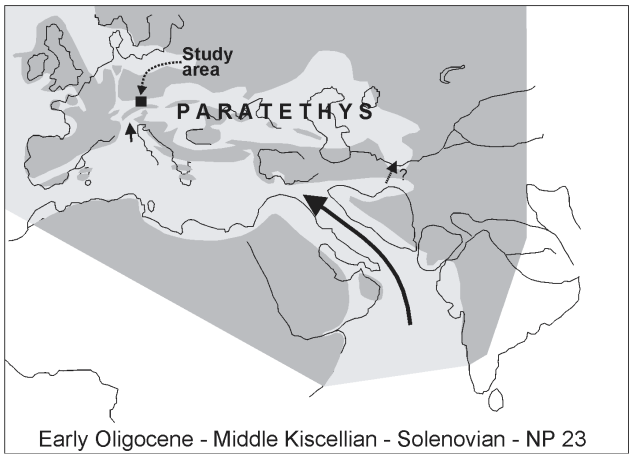

Fig. 1. Paleogeography during nannoplankton Zone NP23 (modified after Rögl 1999) and study area.

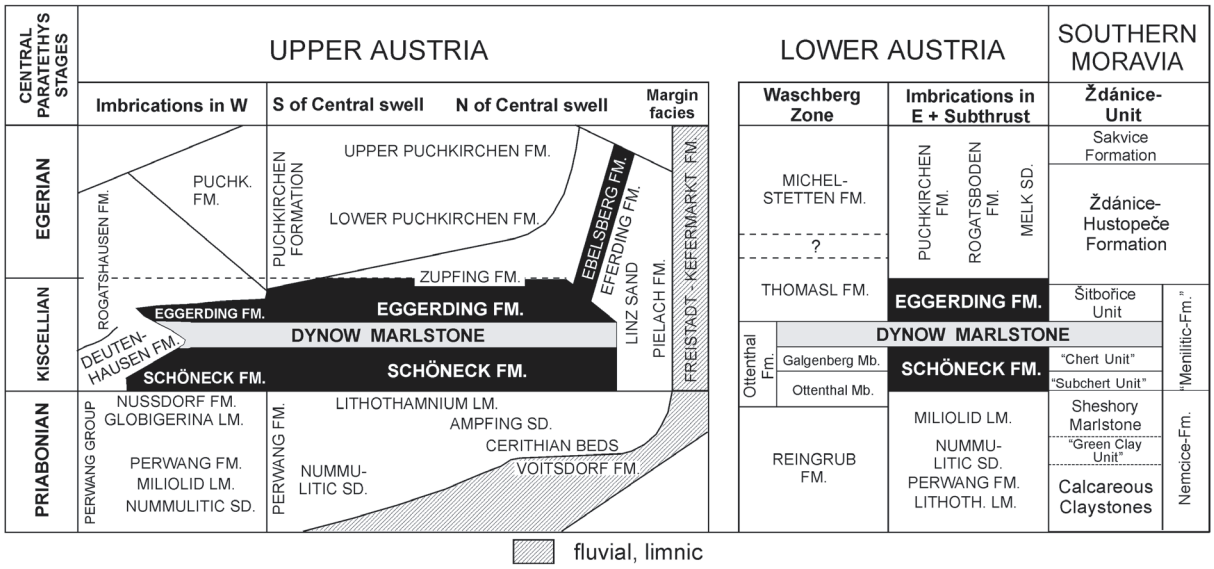

Fig. 2. Stratigraphic sketch of the Eocene/Oligocene transition from the Austrian Molasse Basin to the Carpathian Foredeep (modified after Wagner 1988). The sections for the Waschberg Zone and the Ždánice Unit are from Krhovský et al. (2001).

Accumulation of organic-rich rocks was only temporarily interrupted during the middle part of NP23, when light coloured marls and marly carbonates (Dynow Marlstone, formerly Heller Mergelkalk; Wagner 1998) representing short-term paleoceanographic changes of less than 2 m.yr. (Krhovský et al. 2001) were deposited.

The Dynow Marlstone was first described from the Polish part of the Western Carpathians (Kotlarczyk 1979) and is documented now in the German and Austrian Molasse Basin, along the entire Carpathian Flysch Belt and in the Transylvanian Basin (Krhovský et al. 1991; Popov et al. 1993; Rögl et al. 1997; Rusu et al. 1996). Nevertheless, a formal lithostratigraphic definition is missing.

Detailed studies of the Dynow Marlstone were performed in the Waschberg Zone (Lower Austria; Rögl et al. 2001) and in the Ždánice Unit of the Western Carpathians (Krhovský & Djurasoinovic 1993; Krhovský 1995; Krhovský et al. 2001). There, typical features of the Dynow Marlstone are monospecific, low-salinity tolerant nannoplankton (and diatoms) and tiny endemic (brackish) bivalves. The lack of benthic organisms indicates bottom water anoxia. Surface water salinities below 27 ‰ have been referred to a higher runoff water supply (Budilova et al. 1992).

High-resolution data of the Dynow Marlstone from the western Central Paratethys in Upper Austria are not available yet. Therefore, in the present study vertical lithological and sedimentological variations of a 5.5 m thick succession cored by a borehole (Oberschauersberg 1) in the Upper Austrian Molasse Basin are recorded together with organic geochemical proxies and C–N isotopes of the organic material. Main aims of the study are (1) to examine the paleoceanographic changes in the western Central Paratethys, which resulted in the accumulation of carbonate-rich, organic-poor rocks intercalated between prolific hydrocarbon source rocks, and (2) to compare the factors controlling the deposition of the Dynow Marlstone in the Upper Austrian Molasse Basin with those prevailing in the Western Carpathians.

Regional geology

The study area is located in the Austrian part of the Molasse Basin (Fig. 3), an east–west trending foreland trough, which resulted from the subduction of the southern margin of the European plate beneath the Adriatic plate (Ziegler 1987). The basement is formed by crystalline rocks of the Bohemian Massif covered by autochthonous sediments of Jurassic and Cretaceous age. Sedimentation within the Molasse Basin lasted from Late Eocene to Miocene times. The southern part of the Molasse Basin was overridden by the Alpine nappes (Flysch and Helvetic units, Calcareous Alps) and was included within the overthrust system.

Sedimentation in the Molasse Basin commenced during the Late Eocene in non-marine and shallow-marine environments, which graded southwards into the deeper marine Helvetic realm and the 3000 m deep Flysch Basin. At the Eocene/Oligocene transition the Molasse Basin subsided rapidly to deep-water conditions which resulted in a pronounced change in depositional environments. The changes included the extinction of a carbonate platform with algal reefs (Bachmann et al. 1987), the beginning of slope currents and the deposition of the organic matter-rich Schöneck Formation on the northern basin slope (NP19–20 to lower part of NP23; Schulz et al. 2002).

According to Schulz et al. (2002), deposition of the Schöneck Formation terminated when decreasing surface water salinity caused a break-down of water column stratification and allowed oxygenation of the water body. The overlying organic-lean Dynow Marlstone (NP23; Rögl 1999) is typically about 5 m thick (Fig. 3), but may reach a thickness of up to 15 m. In general, it is described as a light-coloured marlstone originating from pure nannofossil chalk (the first evidence of coccoliths was given by Müller & Blaschke 1971) deposited in a basin with reduced salinity (Báldi 1984; Rögl 1999) and high nutrient content (Rögl et al. 2001). After deposition of the Dynow Marlstone, favourable conditions for the accumulation

of organic matter-rich sediments recurred during Late Kiscellian to Early Miocene times resulting in the deposition of the organic-rich Eggerding (formerly Bändermergel; Wagner 1998) and Ebelsberg Formations (formerly Älterer Schlier; Wagner & Wessely 1997; Wagner 1998; Fig. 2).

Materials and methods

The study is based on core material from the well Oberschauersberg 1 (Osch1; Fig. 2) drilled in 1985 by Rohöl-Aufsuchungs AG (RAG, Vienna), which recovered a complete succession of the Dynow Marlstone including the Schöneck Formation at the base and the Eggerding Formation at the top. A previous study on the Schöneck Formation showed that the Dynow Marlstone in this well is immature ($R_r < 0.35$ %; Schulz et al. 2002). Additional core material from wells Fischlham 1 (Fi1, 1970), Dietach 1 (Di1, 1972) and Rappersdorf 2 (Ra2, 1977; Fig. 3) representing the lowermost part of the Dynow Marlstone was inspected. Sonic logs of these wells and the wells Hochburg 1 (Hobg1, 1985) and Oberhofen 1 (Obhf1, 1982) were provided by RAG for correlation purposes (Fig. 3).

The cores were described, photographed, and sampled in detail. Samples were analysed by means of thin sections and scanning electron microscopy (SEM). Maceral analysis was performed by incident and blue light excitation and point counting transects (400 points per sample).

Powdered samples were analysed for total sulphur (S), total carbon (TC), and organic carbon contents (TOC, after acidification of samples to remove carbonate) using a Leco CS-225 analyser. The difference between TC and TOC is the total inorganic carbon (TIC). Calcite is the only carbonate mineral present. Therefore, calcite contents were calculated using the formula TIC*8.33. Pyrolysis measurements were performed using a Rock-Eval 5 instrument.

After removing carbonates by 2 N HCl, powdered samples were analysed simultaneously for δ^{13}TOC and $\delta^{15}N_{tot}$ with a Thermo/Finnigan MAT Delta plus isotope ratio mass spectrometer, coupled to a Thermo NA 2500CN elemental analyser via a Thermo/Finnigan Conflo II interface. The reference gas was pure N_2 and CO_2 from a cylinder calibrated

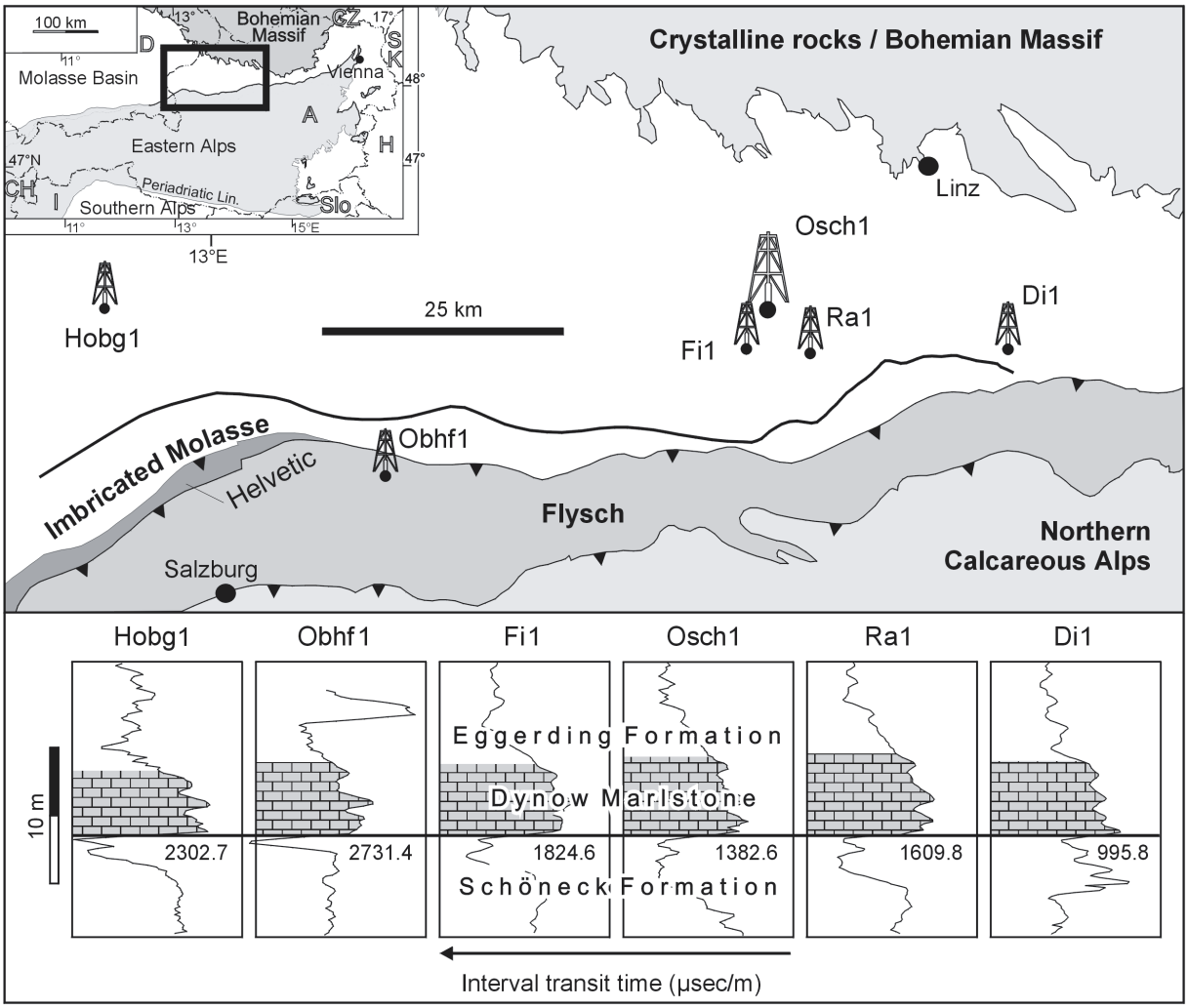

Fig. 3. Geological situation of the study area and site of wells Fischlham 1 (Fi1), Dietach 1 (Di1), Rappersdorf 2 (Ra2), Hochburg 1 (Hobg1), Oberhofen 1 (Obhf1), and Oberschauersberg 1 (Osch1) which recovered a complete succession of the Dynow Marlstone. Below: Sonic log patterns of the Dynow Marlstone.

against IAEA standards N-1 and N-2 and carbonate (NBS-18, NBS-19), respectively. The isotopic results are expressed in the usual delta notation $\delta^{13}C_{TOC}$ or $\delta^{15}N_{tot}$. The standard deviation of the isotope analyses was better than 0.15%. Bulk rock nitrogen isotopes $\delta^{15}N_{tot}$ may closely represent those values expected from organic nitrogen in organic-rich sediments (Calvert et al. 1996; Caplan & Bustin 1998). Most of the nitrogen resides in organic matter according to the very good correlation between TOC and N_{tot} ($r^2 = 0.91$).

As for organic geochemical analyses, portions of the pulverized samples were extracted for approximately 1 h using dichloromethane in a Dionex ASE 200 accelerated solvent extractor at 75 °C and 5 MPa. After evaporation of the solvent to 0.5 ml total solution in a Zymark Turbo Vap 500 closed cell concentrator, asphaltenes were precipitated from a hexane-dichloromethane solution (80 : 1) and separated by centrifugation. The fractions of the hexane-soluble organic matter were separated into saturated hydrocarbons, aromatic hydrocarbons and NSO compounds by medium-pressure liquid chromatography using a Köhnen-Willsch MPLY instrument (Radke et al. 1980).

The saturated and aromatic hydrocarbon fractions were analysed by a gas chromatograph equipped with a 25 m DB-1 fused silica capillary column (i.d. 0.25 mm) and coupled to a Finnigan MAT GCQ ion trap mass spectrometer. The oven temperature was programmed from 70 to 300 °C at a rate of 4 °C min^{-1} followed by an isothermal period of 15 min. Helium was used as carrier gas. The mass spectrometer was operated in the EI (electron impact) mode and a scan range from 50 to 650 daltons (0.7 s total scan time). Data were processed with a Finnigan data system. Identification of individual compounds was accomplished by retention time in the total ion current (TIC) chromatogram and by comparison of the mass spectra with published data. Absolute biomarker concentrations in the saturated and aromatic hydrocarbon fractions were calculated using peak areas from the gas chromatograms in relation to that of internal standards. The concentrations were normalized to the TOC content.

Sedimentology and diagenesis

The Dynow Marlstone in well Osch1 represents a heterogeneous sedimentary unit with a sharp lower boundary towards the Schöneck Formation and a gradual transition into the Eggerding Formation at the top (Figs. 3, 4, 5). The lower boundary is developed as a 2 cm thick interval with rapidly upward increasing carbonate contents, which grades into a massive whitish mudstone (according to DUNHAM's carbonate classification) about 35 cm thick (Fig. 5). This type of massive whitish mudstone recurs one meter above. Apart from the mudstone layers, the Dynow Marlstone is predominantly composed of laminated to wavy bedded white limy marlstones to dark grey silty marlstones (Fig. 4). The upper boundary of the Dynow Marlstone is poorly defined, because an increasing portion of laminated, dark grey marlstones forms a transitional interval to the Eggerding Formation. In Figs. 4 and 5 the upper boundary of the Dynow Marlstone is drawn at the top of the uppermost relatively bright, carbonate-rich marlstone.

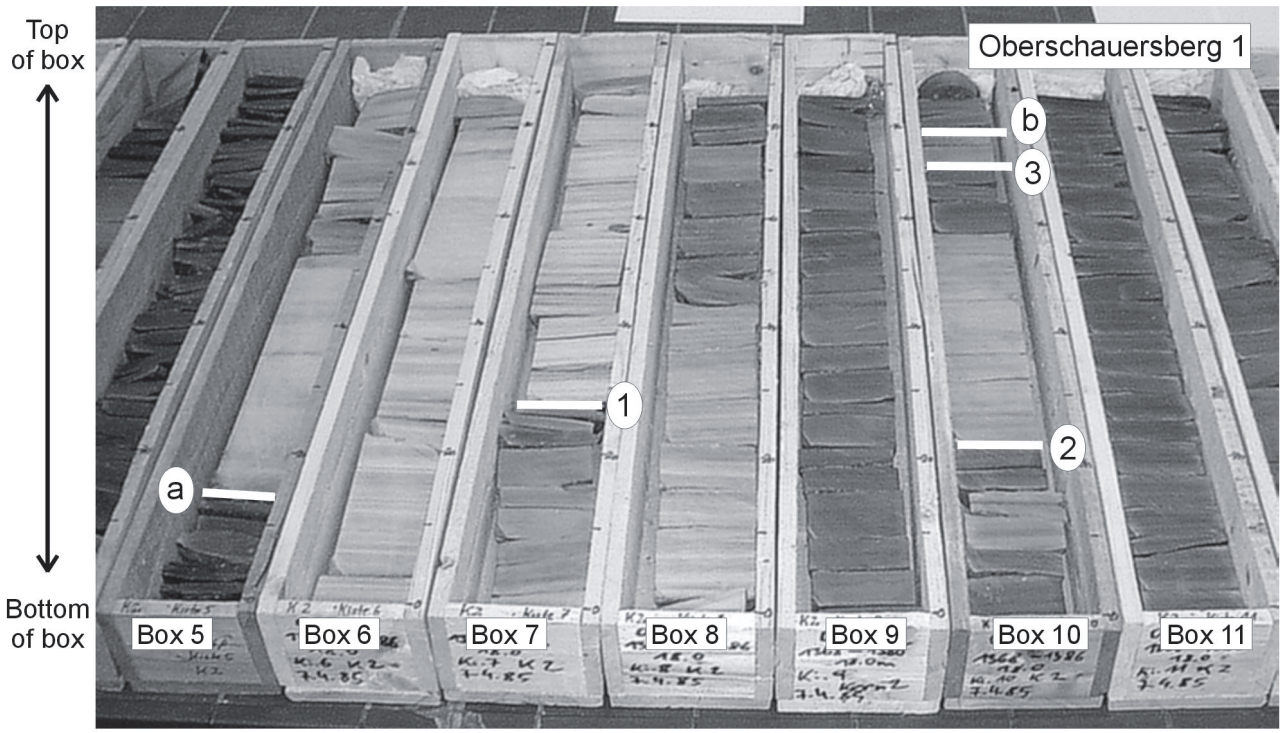

Fig. 4. Core intervals of the Dynow Marlstone with Schöneck Formation at the base and Ebelsberg Formation on the top. **a** — Transition of Schöneck Formation to Dynow Marlstone, **b** — Transition of Dynow Marlstone to Eggerding Formation. **1, 2, 3** — Top of cycles in the Dynow Marlstone. Note difference between upper cycle and boundary between Dynow Marlstone and Eggerding Formation (see also text).

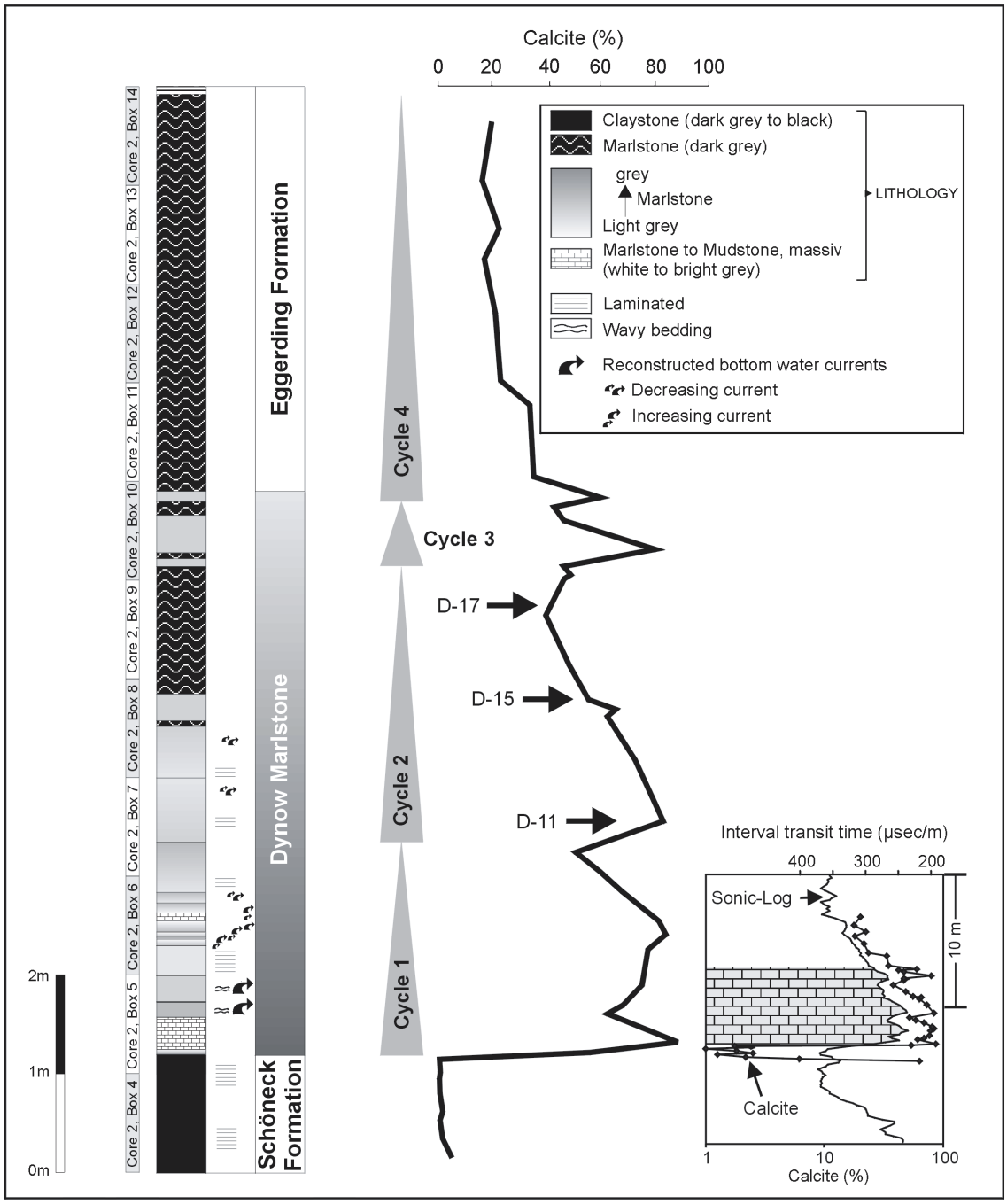

Fig. 5. Lithological sketch, calcite content and sonic log pattern of the Dynow Marlstone in well Oberschauersberg 1. Cycle classification is based on calcite contents (in detail in Fig. 8). Samples D-11, D-15 and D-17 in cycle 2 were investigated for calcareous nannoplankton.

Calcite contents show an overall upward decreasing trend and suggest that the different lithologies occur within several cycles (Figs. 4, 5). Each cycle starts with massive to laminated, whitish mudstones and grades continuously into dark grey mudstones that contain fine-silty quartz (Fig. 6). Wavy lamination occurs within the first cycle and to a lesser extent in the second cycle. The third and fourth cycle (lower part of Eggerding Formation) are characterized by more or less laminated layers. Wavy bedding characteristics within the lower Dynow Marlstone indicate an intensified bottom water current regime. Massive mudstones (nannochalks in origin) at the base and within the first cycle lack irregular bedding characteristics, due to intensive recrystallization. In general, an increase of siliciclastic input (mainly clay and fine silt-sized quartz) correlates with wavy to disruptive bedding characteristics.

Besides very rarely occurring glauconite, phosphatic particles from organic debris are frequently distributed throughout the Dynow Marlstone.

The Dynow Marlstone and the overlying Eggerding Formation contain framboidal pyrite, which is predominantly small-sized and unimodally distributed. The distribution pattern is

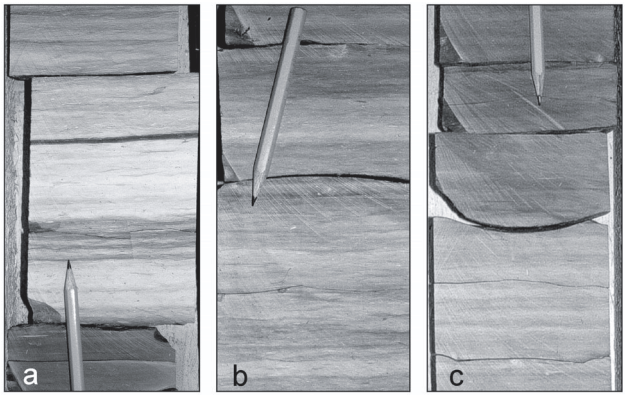

Fig. 6. Sedimentary development of cycle 2 in Dynow Marlstone in well Oberschauersberg 1. **a** — Transition from well-bedded bituminous marlstone to well-bedded white to light grey marlstone with distinct bituminous silty marlstone layers. Core 2, Box 7, 32–54. **b** — Intercalation of grey and dark grey bituminous silty marlstones with slightly wavy bedding. Core 2, Box 8, 10–32. **c** — Transition from well-bedded grey marlstone to well-bedded dark grey marlstone. Core 2, Box 8, 40–60.

characterized by mean sizes between 3 and 4 µm and a standard deviation (σ) of less than 3 µm (Fig. 7). Size distributions of framboidal pyrite have been applied to reconstruct the oxygenation state of depositional environments (Wilkin et al. 1996). Framboid nucleation and growth of pyrite within an anoxic water column in euxinic environments are generally shorter than in sediments with anoxic pore waters. Thus, unimodal-distributed small pyrite framboids in the Dynow Marlstone and the transition to the Eggerding Formation reflect crystallization within an anoxic bottom water column.

Similar pyrite framboid distributions have been found in the middle and upper part of the Schöneck Formation (e.g. "I" in Fig. 7; approx. 1.5 m below the top of the Schöneck Formation). During deposition of the uppermost part of the Schöneck Formation, brackish water conditions resulted in a break-down of water stratification (Schulz et al. 2002). This is reflected by larger framboidal pyrites and by distributions with a higher standard deviation ("II"; "III"). Sample "IV" in Fig. 7 marks the re-establishment of an anoxic bottom water body, which prevailed during deposition of the Dynow Marlstone and the Eggerding Formation.

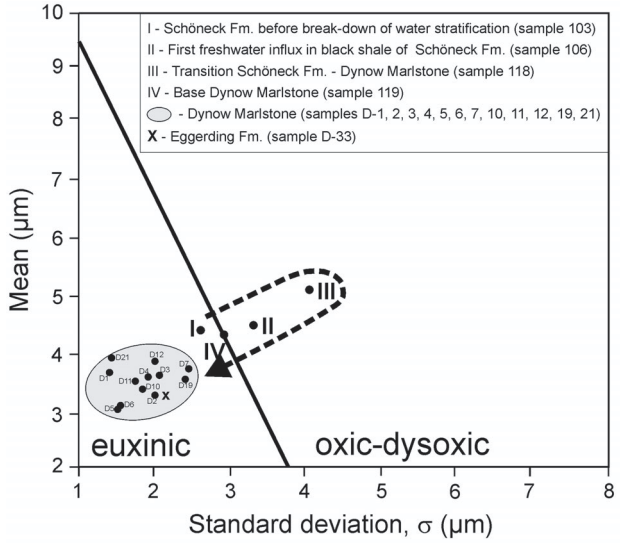

Fig. 7. Mean framboid diameter vs. standard deviation (σ) of the pyrite diameter (according to Wilkin et al. 1996) in Dynow Marlstone and transitions to the top and bottom (well Oberschauersberg 1). See Fig. 8 for sampling.

Log correlation

The insert in Fig. 5 shows that in the case of the Dynow Marlstone and the lower Eggerding Formation, the interval transit time recorded by the sonic log is mainly a function of carbonate contents. Therefore, the sonic log can be used to correlate limestone layers. The (marly) limestone beds forming the base of cycles 1, 2 and 4 are clearly visible in the logs (Fig. 3), but a separation between cycles 3 and 4 is barely possible. In some logs the upper limestone layer in cycle 1 can be distinguished.

In well Obhf1 the Dynow Marlstone is missing in the autochthonous Molasse section. However, Dynow Marlstone occurs in this well at a depth of about 2730 m in allochthonous Molasse imbricates (Wagner et al. 1986; Fig. 3). According to palinspastic reconstructions by Wagner (1998), these sediments were deposited at least 30 to 65 km south of their present-day position.

The sonic logs presented in Fig. 3 document that the Dynow Marlstone continues laterally. The major cycles 1, 2 and 4 can be traced over roughly 100 km in an E–W direction (Di1–Hobg1) and at least 50 kilometers in a N–S direction. This clearly proves that the mechanisms controlling the cyclic structure of the Dynow Marlstone and the lower Eggerding Formation were effective on a basin-wide scale.

Organic petrography and proxies of the organic material

The TOC contents in the Dynow Marlstone range from 0.5 to 2 % (Fig. 8), while within the studied interval of the Eggerding Formation they are up to 3.5 %. The TOC contents are closely related to cycles 1 to 4 with upward increasing TOC contents within each cycle. There is a strong negative correlation between TOC and calcite (correlation coefficient $r^2 = 0.79$; Fig. 9) which, according to Ricken (1991), indicates roughly constant production of organic matter and dilution by varying amounts of calcite. Calcite in the studied section is mainly derived from calcareous nannoplankton, suggesting a negative correlation between TOC contents and algal blooms.

The organic petrographic composition of the Dynow Marlstone is related to the lithology of the host rock. The massive mudstones at the base of the first two cycles contain exclusively bituminite (petrographic association "I" in Fig. 8). Grey marlstones are also dominated by bituminite, but include minor amounts (<5 vol. % of total visible organic matter) of small alginite and detrital liptinite, huminite and inertinite, (association "I–II"). Alginite and humodetrinite percentages are above 5 vol. % in association "II", which occurs in dark

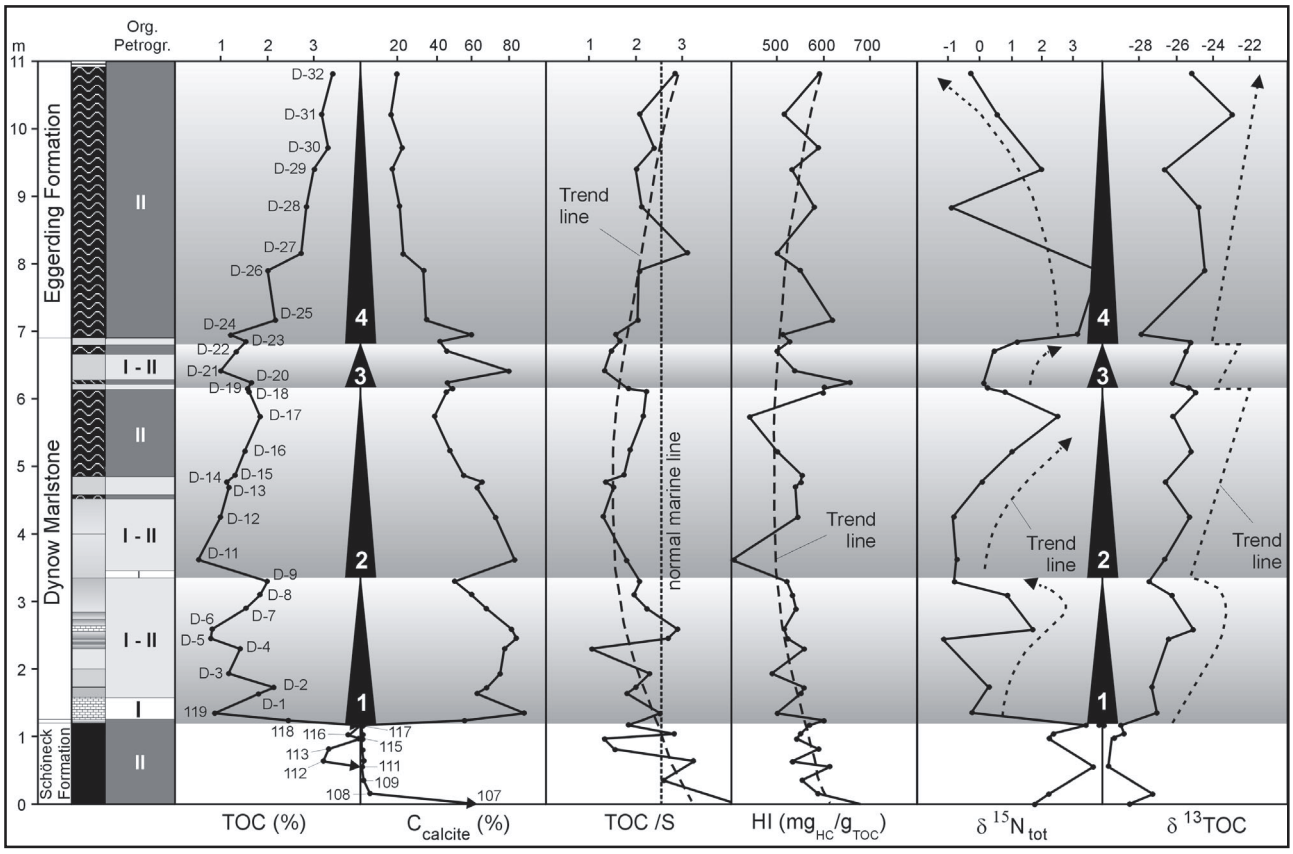

Fig. 8. Organic geochemical proxies, organic petrography and C-N isotopes in Dynow Marlstone and transitions to the top and bottom (well Oberschauersberg 1). **1–3** — cycles within Dynow Marlstone, **4** — cycle leading to permanent depositional conditions of the Eggerding Formation. Roman numbers **I**, **I–II** and **II** in the field for organic petrography are explained in the text. Sampling and sample numbers are indicated in the field for TOC.

grey marlstones in the upper part of the Dynow Marlstone and in the Eggerding Formation. Thus, a slight but progressive input of terrestrial organic material into the depositional setting can be recorded.

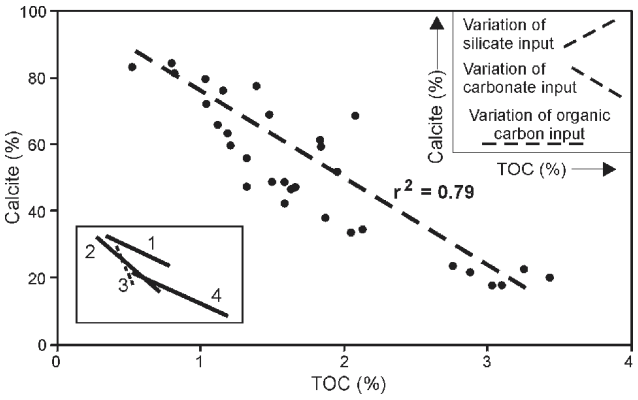

Fig. 9. TOC vs. calcite content in Dynow Marlstone and Eggerding Formation in well Oberschauersberg 1. Insert in the upper right corner shows type of deposition reflected by different relationships between TOC and calcite (simplified after Ricken 1991). Note insert in the lower left corner: TOC-Calcite plots for single cycles (1–4) yield similar regression lines and prove decreasing carbonate input from cycle 1 to cycle 4.

Most hydrogen index values (HI) fall in the range between 500 and 600 mg_{HC}/g_{TOC}. TOC/S ratios vary from 1 to 3 (Fig. 8). The trend lines for both proxies highlight a continuous decrease within the lower part of the Dynow Marlstone and a continuous increase within the uppermost part and within the Eggerding Formation.

Because there is no indication for massive changes in organic matter input, the slightly reduced HI values in the middle part of the section may be due to intensified bacterial overprint of the organic material during deposition of the Dynow Marlstone. Suppressed TOC/S ratios point to more effective sulphate reduction and support this hypothesis. The observed TOC/S ratios <2.8 furthermore indicate anoxic bottom water conditions (Berner 1984; Berner & Raiswell 1983).

Biomarkers and C–N isotopes of the organic material

After a significant drop across the base of the Dynow Marlstone, pristane/phytane ratios increase slightly upwards from about 2 to 3 (Fig. 10). Pristane/phytane ratios are known to be affected by maturation (Tissot & Welte 1984) and by differences in the precursors for acyclic isoprenoids (i.e. bacterial origin; Volkman & Maxwell 1986; ten Haven et al. 1987). An influence of different maturity on pristane/phytane ratios can

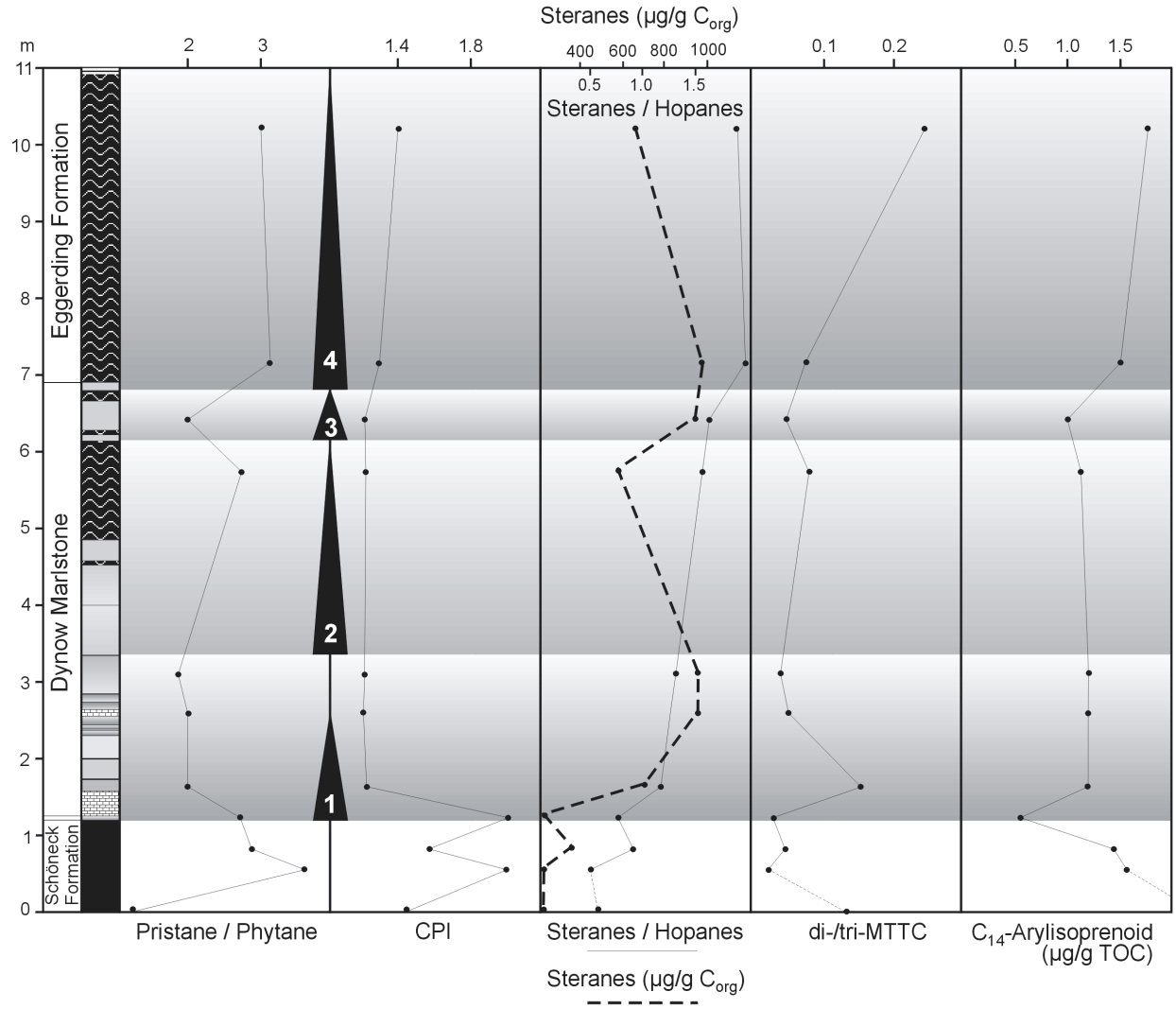

Fig. 10. Carbon preference index (CPI), pristane/phytane and steranes/hopanes ratios, and concentrations of 4-methylsteranes, tri-MTTC and C_{14}-arylisoprenoid in the Dynow Marlstone and transitions to the top and bottom (well Oberschauersberg 1).

be ruled out, due to the low vertical distance of the samples within the investigation profile in well Osch1 (about 6 m). The low maturity at Osch1 ($R_r < 0.35$ %) further argues against the formation of pristane from tocopherols (vitamin-E) or chromanes (Goossens et al. 1984). However, a bacterial origin of phytane from phytanyl ether lipids found in archaebacteria cannot be excluded (Volkman & Maxwell 1986; ten Haven et al. 1987). According to previous studies (Didyk et al. 1978), an increase in pristane/phytane ratios would indicate the establishment of more oxic conditions in the bottom water during sedimentation. This interpretation contradicts the increase in C_{14}-arylisoprenoid concentrations (Fig. 10; see below).

Aryl isoprenoids are thought to be derived from the carotenoid isorenieratene, which is specific for the photosynthetic green sulphur bacteria Chlorobiaceae and purple sulfur bacteria Chromatiaceae (Summons & Powell 1987). These organisms are phototrophic anaerobes and, thus, require both light and H_2S for growth. In modern environments they appear in sulphate-containing water bodies that are sufficiently quiescent and organic-rich to enable sulphide production close to the photic zone (Summons 1993). Euxinic conditions in the deep water zone are required, and the intensity of the green spectral component of the light used for photosynthesis should be reduced by particulate organic matter or vegetation in the water column (Pfennig 1977). Besides the lowermost sample, the concentration of aryl isoprenoids remains rather constant within the Dynow Marlstone and increases in the Eggerding Formation. Increasing concentrations may also be due to a rising chemocline (Repeta 1993; Sinninghe-Damsté et al. 1987b).

Constant values of the carbon preference index (CPI, calculated after Bray & Evans 1961) throughout the Dynow Marlstone and along the transition to the Eggerding Formation (Fig. 10) point to similar sources of humic material, which is abundant in different concentrations (see organic petrography). Furthermore, the percentages of saturated and aromatic hydrocarbons, NSO compounds and asphaltenes remain constant throughout the investigated profile (18 : 15 : 50 : 17) and indicate a rather similar organic matter composition.

A trimethylated 2-methyl-2-trimethyl-tridecylchroman (C_{29}-chroman; tri-MTTC) occurs in significant amounts and

has been identified by comparison of the mass spectrum with published data (Sinninghe Damsté et al. 1987a; Schwark & Püttmann 1990; for a review about chroman geochemistry see Schwark et al. 1998). The corresponding dimethylated compound (di-MTTC) has also been found in very low intensities in the aromatic hydrocarbon fractions of the sediment samples. The predominance of tri-MTTC over its dimethylated counterpart is indicative for mesohaline to euhaline (30–40 ‰) conditions. Chroman assemblages dominated by di-MTTC were found in sediments deposited under hypersaline conditions (Sinninghe Damsté et al. 1987a; Schwark & Püttmann 1990). Except for one outlier at the base, the ratio of both biomarkers (di-/tri-MTTC) remains on a fairly constant level of less than 0.1 throughout the Dynow Marlstone (Fig. 10). A value of more than 0.2 recorded in the lower Eggerding Formation suggests an important increase in salinity.

Other constituents of the saturated hydrocarbons are αβ- and βα-hopanes from C_{27} to C_{35}, but the C_{28} hopanes are absent. Hopanoids have been identified as membrane constituents in many procaryotes (e.g. bacteria) including some growing anaerobically (Ourisson et al. 1979).

Steroids are dominated by 5α-steranes from C_{27} to C_{29} and minor amounts of 5β-steranes, as well as 4α-methylsteranes. The predominant primary producers of sterols are phytoplankton and photosynthetic bacteria living in the photic zone of the water column (Volkman 1986). Sterane concentrations increase in cycle 1 of the Dynow Marlstone indicating increased sterol productivity and remain on a rather constant level in the upper part of the section.

The steranes/hopanes ratio increases upwards slightly but constantly from about 1 to 2 (Fig. 10). High steranes/hopanes ratios (up to 3) in the lower part of the Schöneck Formation were interpreted as consistent with full-marine conditions (Schulz et al. 2002). Furthermore, increasing steranes/hopanes ratios in the German Kupferschiefer reflect an increasing marine influence during the initial Zechstein transgression (Bechtel & Püttmann 1997). Additionally, variations of the steranes/hopanes ratio can be attributed to fluctuations of the trophic level during deposition of the Schöneck Formation (Schulz et al. 2002). Thus, an increase of this ratio in the investigated profile points either to increasing nutrient contents or to the establishment of normal marine conditions.

$\delta^{13}C$ values in the studied section range from –30 to –23 ‰ and show an upward trend towards heavier values (Fig. 8). Because organic carbon of terrigenous material is typically isotopically lighter (~ –27 ‰) than marine organic material (~ –21 ‰; Meyers 1994), the measured $\delta^{13}C$ values may reflect a mixed organic matter source. The trend towards heavier values parallels the change from petrographic association I dominating in the lower part of the Dynow Marlstone to petrograpic association II prevailing in the Eggerding Formation (Fig. 8) and may be triggered by the change from brackish to fully marine conditions in the Eggerding Formation (see di-/tri-MTTC ratio in Fig. 10). According to Schulz et al. (2002), the very light $\delta^{13}C$ values at the top of the Schöneck Formation result from CO_2 recycling.

Small-scale cyclic variations, each with a tendency to higher values at the top, exist within the general tendency to heavier $\delta^{13}C$ values. As the sterane concentrations data for the first cycle indicate an increase in primary sterol productivity (Fig. 10), heavier $\delta^{13}C$ signals may reflect CO_2 limitation and less fractionation during CO_2 uptake. This phenomenon can be explained by the reduced buffering capacity of carbonate systems with low salinity water, which leads to an increase in pH during high primary productivity periods (Voß & Struck 1997). However, the sterane concentrations remain on a fairly constant level throughout the following cycles 2–4 (Fig. 10). Thus, intra-cycle variations to heavier $\delta^{13}C$ values may be contingent on an increased amount of marine organic material.

$\delta^{15}N$ data in the Dynow Marlstone cycle 1 scatter widely (Fig. 8). In contrast, the cycles 2 and 3 reveal clear trends with upward increasing values, whereas cycle 4 exhibits a (weak) trend towards lighter values. $\delta^{15}N$ values of sedimentary organic matter reflect integrated signals of various factors. First, they can be used to distinguish between organic matter derived from algae and land-plants (Meyers 1997). Atmospheric N_2 ($\delta^{15}N$ about 0 ‰) is the nitrogen source for terrestrial plants, whereas dissolved nitrate with heavier $\delta^{15}N$ values is the nitrogen source for plankton. Land-plants, therefore, are characterized by lower $\delta^{15}N$ values. Second, high nutrient concentrations in surficial waters lead to the production of organic matter with low $\delta^{15}N$ values, because faster uptake kinetics cause preferential assimilation of ^{14}N (relative to ^{15}N) when nutrients are abundant. Third, the totally different interpretation invoking diagenetic alteration of nitrogen isotopic ratios in the presence of oxygen (cf. Sachs & Repeta 1999 and references herein) can be excluded, because C_{14}-aryl-isoprenoids (Fig. 10) indicate permanent bottom water anoxia throughout deposition of the studied profile. Thus, the observed trends in cycles 2 and 3 reflect either increasing contents of plankton, or — more likely — decreasing N-isotope fractionation because of decreasing nutrient availability. Isotopic fractionation due to partial utilization of dissolved inorganic nitrogen may account for the tendency towards lighter $\delta^{15}N$ values within cycle 4 (according to Altabet & Francois 1994).

Paleoceanographic implications

In the Upper Austrian Molasse Basin, the Dynow Marlstone, about 5 m thick, is interbedded between two organic-rich formations (Schöneck and Eggerding Formation). The rock unit, relatively poor in organic matter, represents a major break in the evolution of the Paratethys. In some wells the Dynow Marlstone is missing (e.g. the autochthonous part of Obhf1), perhaps because of submarine erosion or slumping. Furthermore, this sedimentary unit is not described from marginal basin connections (Upper Rhine Valley, Lower Inn Depression, Slovenian Corridor; Ortner & Sachsenhofer 1996; Schmiedl et al. 2002; Doebl 1970). Nevertheless, the lateral continuity of this unit is remarkably high, arguing for tectonically stable conditions.

Nannoplankton of three samples from the second cycle in the Dynow Marlstone have been described by Báldi-Beke (2003; see Fig. 5 for position of samples). In general, the nannoplankton diversity is poor, but indicative of the nannoplankton Zone NP23. *Reticulofenestra ornata* predominates. This species formed blooms during NP23 and NP24, but has a range from NP22 to NP25. At the top of cycle 2 *Transversopontis fibula* has been identified, which is characteristic for

the lowermost NP23. The *Transversopontis fibula-Reticulofenestra ornata* assemblage ("olbinian-type nannoflora") has been described as characteristic for the Central and Eastern Paratethys and may indicate brackish water conditions (Nagymarosy & Voronina 1992).

Transversopontis fibula is often related to a level to endemic bivalves ("*Cardium lipoldi*"-fauna) and ostracods (Cyprididae), a fact which enables correlations throughout the entire Paratethys (Popov et al. 1993). This marker horizon has been described from the Dynow Marlstone in the Waschberg Unit (Rögl et al. 2001) and the Carpathians (Krhovský et al. 2001), but is not present in well Osch1.

Reticulofenestra ornata also predominates in the lower part of the Eggerding Formation, whereas *Transversopontis fibula* was not found. This phenomenon has been referred to a strong salinity decrease (Nagymarosy & Voronina 1992). However, this interpretation is in conflict with increasing di-/tri-MTTC ratios (Fig. 10), which point to increasing salinities.

According to our results, oligotrophic conditions prevailed and surface water salinities decreased during the final stages of the deposition of the Schöneck Formation. Decreasing salinities were referred to increasing fresh water ingressions. Furthermore, the end of CO_2 recycling was referred to a break-down of water stratification (Schulz et al. 2002). Pyrite framboid diameters suggest a short time interval with dysoxic (to oxic?) conditions (Fig. 7). However, detectable C_{14}-arylisoprenoids across the transition and within the complete Dynow Marlstone advocate for persistent photic zone anoxia (Fig. 10).

Cartoons illustrating different processes, active during deposition of the Dynow Marlstone and the lowermost Eggerding Formation are presented in Figs. 11a and 11b, respectively. With the onset of Dynow Marlstone sedimentation, an abrupt increase in nutrients favoured an abrupt return to the eutrophic conditions that earlier had occurred during deposition of the lower Schöneck Formation. Eutrophic conditions continued until the deposition of the Eggerding Formation. The high primary production level during deposition of the Dynow Marlstone promoted cyclic blooms of calcareous nannoplankton.

This scenario favoured nitrogen fixation ($\delta^{15}N$ = –1 to +4; Fig. 8). Variations of the $\delta^{15}N$ signals to heavier values within the single cycles are referred to diminished N-isotope fractionation probably due to decreasing nutrient supply. However, the primary organic carbon productivity remained fairly constant during deposition of the Dynow Marlstone (sterane concentrations in Fig. 10). The different $\delta^{15}N$ values are not useful source indicators (land plant vs. plankton) in the case of the Dynow Marlstone. Questions remain regarding the extent of denitrification and anaerobic oxidation of ammonia in the anoxic water column during deposition of the Dynow Marlstone ("anammox reaction"; Kuypers et al. 2003; Dalsgaard et al. 2003).

A shift to heavier carbon isotope values within the single cycles indicates increasing portions of marine organic material. Thus, stronger CO_2 reduction during enhanced primary production resulting from eutrophication and high primary production in low salinity water can be excluded (Voß & Struck 1997). Preservation of the organic material was enhanced by contemporaneously establishing anoxic bottom water. On the other hand, intensive sulphate reduction lowered the hydrogen index in the upper part of the Dynow Marlstone. Due to the lack of reactive iron within the pore water, pyrite formation was depressed and hydrogen sulphide escaped into the bottom water.

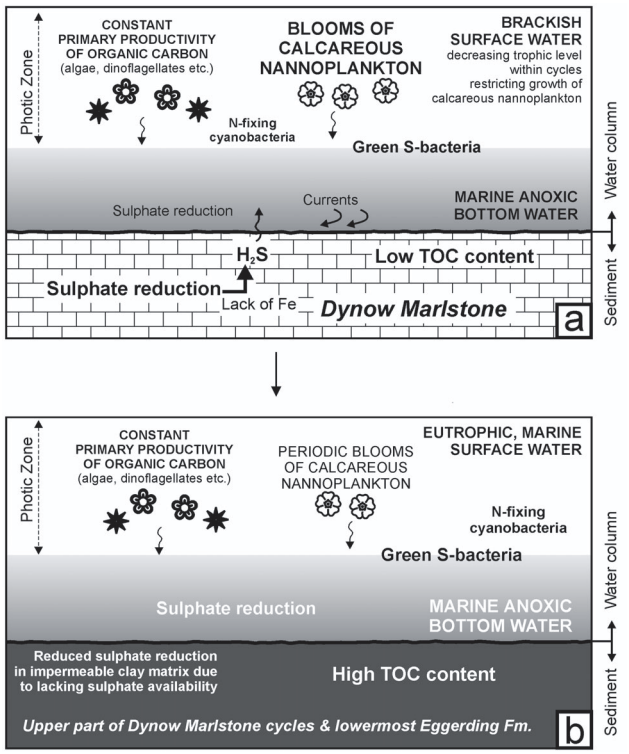

Fig. 11. Depositional model for the Dynow Marlstone (**a**) and the upper part of the Dynow Marlstone cycles and the lowermost Eggerding Formation (**b**) in well Oberschauersberg 1. The accumulation of the Dynow Marlstone was controlled by periodical blooms of calcareous nannoplankton (a). The produced carbonate dilutes the organic matter in the sediments and results in varying and relatively low TOC contents. Nannoplankton blooms were caused by high trophic levels probably related to fresh water ingressions. Contemporaneously, bottom currents reworked the sediment and led to fluctuations of sulphate reduction intensity due to limited sulphate availability. The primary productivity of organic carbon remained roughly constant and anoxic bottom water conditions favoured organic matter preservation during the deposition of the Dynow Marlstone and Eggerding Formation. Changes at the transition from the Dynow Marlstone to the Eggerding Formation include intensified photic zone anoxia and an increase in salinity (b).

The organic geochemical data indicate euhaline to mesohaline (30–40 ‰) surface water conditions during deposition of the Dynow Marlstone as tri-MTTC predominates by far over its dimethylated counterpart (Sinninghe Damsté et al. 1987; Schwark & Püttmann 1990). On the other hand, the initial deposition of the Eggerding Formation was coupled to a progressively intensified water stratification and a salinity increase (increasing C_{14}-arylisoprenoid concentrations and di-/tri-MTTC ratios; Fig. 10). The salinity proxy (di-/tri-MTTC ratio) indicates a gradual return to normal-marine conditions, but contradicts the nannoplankton findings (see previous chapter).

Similar environments occurred during deposition of the Dynow Marlstone in the Western Carpathians in the Ždánice Unit (Czechia; Krhovský 1995). There, brackish surface water

and anoxic bottom water conditions were inferred from the paleontological record. In contrast to the Molasse Basin, the Dynow Marlstone in the Ždánice Unit contains silica from diatom frustules. According to Krhovský (1995), the silicified marlstones were deposited during relatively dry climatic periods characterized by high seasonality (hot and dry summers, cool and wet winters) linked to short-term, orbitally forced changes of seasonality within a long-eccentricity orbital cycle. Sandy layers within the upper part of the Dynow Marlstone should indicate a following wetter period, which caused intensified weathering on the Bohemain Massif and stimulated the input of detrital material.

The Dynow Marlstone in the Ždánice Unit is overlain by slumps and pebbles that transfer to the deposition of pelitic rocks (Šitbořice Event; Krhovský 1995). This regional event is considered a consequence of a sea-level fall during eustatic cycle TA 4.5 according to Haq et al. (1987) or of tectonic activity (Krhovský & Djurasoinovic 1993).

Considering the results from the Ždánice Unit, there are three factors that may have influenced the sedimentary change from the Dynow Marlstone to the Eggerding Formation in the Upper Austrian Molasse Basin:

1 — Intensified photic zone anoxia and increasing salinities may have changed the ecological conditions for calcareous nannoplankton and limited the carbonate production. Increasing salinities and a return to full-marine conditions are probably related to the reactivation of the connection of the Paratethys with the open sea (Popov et al. 1993; Popov & Stolyarov 1996).

2 — Climatic changes postulated by Krhovský (1995) caused increased weathering and run-off from the Bohemian Massif and provided enhanced amounts of detrital material. However, this interpretation may be in conflict with the observed rise in salinity during deposition of the Eggerding Formation.

3 — The transition to the Eggerding Formation may be related to the Šitbořice Event (Krhovský 1995). However, this event was not described until now in the Upper Austrian Molasse Basin, and no evidence for slumping or sedimentation in lowstand fans was found in the present study.

Therefore, a basin-wide decline in carbonate production due to ecological changes is the most probable explanation for the observed change from the deposition of bright-coloured calcareous muds to the deposition of dark-coloured (calcareous) shales. This is also in accordance with the observed negative correlation between carbonate and TOC (Fig. 9) showing that organic matter deposition was controlled by the amount of carbonate rather than by the amount of detrital material and explains why this change extended across the whole outer Paratethyan shelf during the second half of NP23.

Conclusions

Massive organic carbon accumulation in the Upper Austrian Molasse Basin was interrupted during NP23 by deposition of the organic-poor intervals of the approximately 5 m thick Dynow Marlstone.

During deposition of the uppermost part of the organic-rich Schöneck Formation, oligotrophic conditions prevailed and surface water salinities decreased. The base of the Dynow Marlstone is characterized by an abrupt increase in primary organic productivity, but persisting photic zone anoxia.

This stable depositional scenario of the Dynow Marlstone was overprinted by cyclic increases in the trophic level favouring blooms of calcareous nannoplankton. Subsequently, trophic levels and the production of calcareous nannoplankton decreased gradually. Within each cycle, the percentage of marine organic material increases. Limestones with low TOC contents, a consequence of the dilution of organic matter by the calcareous nannoplankton, were deposited during algal blooms, whereas organic-rich marls accumulated during periods with low production of calcareous nannoplankton. Sulphate reduction occurred in the sediment as well as in the anoxic bottom water. Hydrogen sulphide generated in the sediment escaped due to the lack of reactive iron. The intensive consumption of labile organic material decreased the hydrogen index.

The cyclic physicochemical conditions were modified after the last major bloom of calcareous nannoplankton (top of Dynow Marlstone). The biomarker data suggest intensified photic zone anoxia (increase of concentrations of C_{14}-arylisoprenoids) coupled to a marked increase in salinity (increase of di-/tri-MTTC; both proxies in Fig. 10). These changes resulted in the deposition of the marls of the Eggerding Formation, characterized by upward increasing TOC contents. Sulphate reduction in impermeable pelites of the Eggerding Formation was limited by sulphate availability.

Acknowledgments: The authors thank Rohölaufsuchungs AG (Vienna) for providing core material and well logs. Technical assistance was given by colleagues at the Geological Departments in Clausthal (Germany) and Leoben (Austria). Special thanks to Fred Rögl, Maria Báldi-Beke and András Nagymarosy, whose help on various aspects of the "Dynow" enhanced our interpretations. Furthermore, the paper benefited greatly from the critical remarks of Alessandra Negri, Ján Soták, and Phil Meyers.

References

Altabet M.A. & Francois R. 1994: Sedimentary nitrogen isotopic ratio as a recorder for surface ocean nitrate utilization. *Global Biogeochemical Cycles* 8, 1, 103–116.

Bachmann G.H., Müller M. & Weggen K. 1987: Evolution of the Molasse Basin (Germany, Switzerland). *Tectonophysics* 137, 77–92.

Báldi T. 1984: The terminal Eocene and Early Oligocene events in Hungary and the separation of an anoxic, cold Paratethys. *Eclogae Geol. Helv.* 77, 1, 1–27.

Báldi-Beke M. 2003: Report on nannoplankton assemblages from the Dynow Marlstone, Upper Austrian Molasse Basin. Üröm April 2003. 1–2 (unpublished).

Bechtel A. & Püttmann W. 1997: Palaeoceanography of the early Zechstein Sea during Kupferschiefer deposition in the Lower Rhine basin (Germany): A reappraisal from stable isotope and organic geochemical investigations. *Palaeogeogr. Palaeoclimatol. Palaeoecol.* 136, 331–358.

Berner R.A. 1984: Sedimentary pyrite formation: An update. *Geochim. Cosmochim. Acta* 48, 605–615.

Berner R.A. & Raiswell R. 1983: Burial of organic carbon and py-

rite sulfur in sediments over Phanerozoic time: A new theory. *Geochim. Cosmochim. Acta* 47, 885–862.

Bray E.E. & Evans E.D. 1961: Distribution of *n*-paraffins as a clue to recognition of source beds. *Geochim. Cosmochim. Acta* 22, 2–15.

Budilová P., Hladíková J. & Krhovský J. 1992: Late Eocene and Early Oligocene planktonic foraminifera and sediments of the Ždánice and Pouzdřany Units: carbon and oxygen isotopic study. *Scripta* 22, 67.

Calvert S.E., Bustin R.M. & Ingall E.D. 1996: Influences of water column anoxia and sediment supply on the burial and preservation of organic carbon in marine shales. *Geochim. Cosmochim. Acta* 60, 1577–1593.

Caplan M.L. & Bustin R.M. 1998: Paleoceanographic controls on geochemical characteristics of organic-rich Exshaw mudrocks: role of enhanced primary production. *Organic Geochemistry* 30, 161–188.

Dalsgaard T., Canfield D.E., Petersen J., Thamdrup B. & Acuña-Gonzalez J. 2003: N_2 production by the anammox reaction in the anoxic water column of Golfo Dulce, Costa Rica. *Nature* 422, 606–608.

Didyk B.M., Simoneit B.R.T., Brassell S.C. & Eglinton G. 1978: Organic geochemical indicators of palaeo-environmental conditions of sedimentation. *Nature* 272, 216–222.

Doebl F. 1970: Die tertiären und quartären Sedimente des südlichen Rheingrabens. In: Illies H. & Mueller S. (Eds.): Graben Problems. *Sci. Rep. Int. Upper Mantle Proj.* 27, Stuttgart, 56–66 (in German).

Dohmann L. 1991: Die unteroligozänen Fischschiefer im Molassebecken. *PhD thesis, Ludwig-Maximilian-Universität,* Munich, 1–365 (in German).

Gerhard J. 1982: Geochemische Untersuchungen an einem potentiellen Erdölmuttergestein. *Gießener Geologische Schriften* 29, 1–191 (in German).

Gerhard J. 1988: Faziesdiagnose und Paläoenvironment des Sannois-Fischschiefers (Alpines Molassebecken, Bayern, Süddeutschland). *DGMK Dtsch. Wissenschaftliche Gesellschaft für Erdöl, Erdgas und Kohle e.V. Berichte* 406, 1–128 (in German).

Goossens H., de Leeuw J.W., Schenck P.A. & Brassell S.C. 1984: Tocopherols as likely precursors of pristane in ancient sediments and crude oils. *Nature* 312, 440–442.

Haq B.U., Hardenbol J. & Vail P.R. 1987: Chronology of fluctuating sea levels since the Triassic. *Science* 235, 115–1167.

ten Haven H., de Leeuw J.W., Rullkötter J. & Sinninghe Damsté J.S. 1987: Restricted utility of the pristane/phytane ratio as a palaeoenvironmental indicator. *Nature* 330, 641–643.

Kotlarczyk J. 1979: Introduction to stratigraphy of the Skole Unit of the Flysch Carpathians. *Badania Palaeontologiczne Karpat Przemyskich* 14–26 (in Polish).

Krhovský J. 1995: Early Oligocene palaeoenvoronmental changes in the West Carpathian Flysch Belt of southern Moravia. 4th Proccedings of the Carpatho-Balcan Geological Association, September 1995, Athens, Greece. *Geol. Soc. Greece, Spec. Publ.* 209–213.

Krhovský J. & Djurasoinovic M. 1993: The nannofossil chalk layers in the early Oligocene Šitbořice Member in Velké Nemčice (the Menilitic Formation, Ždánice Unit, South Moravia): Orbitally forced changes in paleoproductivity. In: Hamršmíd B. (Ed.): Nové výsledky v terciéru Západních Karpat. Sborník referátů z 10. konference o mladším terciéru, Brno, 27.–28.4.1992. *Knihovnička ZPN* 15, 33–53.

Krhovský J., Adamová M., Hladíková J. & Maslowská H. 1991: Paleoenvironmental changes across the Eocene/Oligocene boundary in the Ždánice and Pouzdřany Units (Western Carpathians, Czechoslovakia): the long-term trend and orbitally forced changes in calcareous nannofossil assemblages. In: Hamršmíd B. & Young J.R. (Eds.): Nannoplankton research. Proceed. 4th Internat. Nannoplankton Assoc. Conference, II, *Knihovnička ZPN* 14b, 105–187.

Krhovský J., Rögl F. & Hamršmíd B. 2001: Stratigraphic correlation of the Late Eocene to Early Miocene of the Waschberg Unit (Lower Austria) with the Ždánice and Pouzdřany Units (South Moravia). In: Piller W.E. & Rasser M.W. (Eds.): Paleogene of the Eastern Alps. Österreichische Akademie der Wissenschaften. *Schriftenreihe der Erdwissenschaftlichen Kommissionen* 14, 225–254.

Kuypers M.M.M., Sliekers A.O., Lavik G., Schmid M., Jørgensen B.B., Kuenen J.G., Sinninghe Damsté J.S., Strous M. & Jetten M.S.M. 2003: Anaerobic ammonium oxidation by anammox bacteria in the Black Sea. *Nature* 422, 608–611.

Martini E. 1971: Standard Tertiary and Quarternary calcareous nannoplankton zonation. Proc. 2nd planktonic Conference, Roma 1970. *Ed. Tecnoscienza,* Roma, 739–785.

Meyers P.A. 1994: Preservation of elemental and isotopic identification of sedimentary organic matter. *Chem. Geol.* 144, 289, 302.

Meyers P.A. 1997: Organic geochemical proxies of paleoceanographic, paleolimnologic, and paleoclimatic processes. *Organic Geochemistry* 27, 5/6 213, 250.

Müller G. & Blaschke H. 1971: Coccoliths: Important rock-forming elements in bituminous shales of Central Europe. *Sedimentology* 17, 119–124.

Nagymarosy A. & Voronina A.A. 1992: Calcareous nannoplankton from the Lower Maykopian Beds (Early Oligocene, Union of Independent States). Proc. of the Fourth INA Conference, Prague. *Knihovnička ZPN* 14b, vol. 2, 189–221.

Ortner H. & Sachsenhofer R.F. 1996: Evolution of the Lower Inn Valley Tertiary and constraints on the development of the source area. In: Wessely G. & Liebl W. (Eds.): Oil and gas in Alpidic thrustbelts and basins of Central and Eastern Europe. *EAGE Spec. Publ.* 5, 237–247.

Ourisson G., Albrecht P. & Rohmer M. 1979: The hopanoids: palaeochemistry and biochemistry of a group of natural products. *Pure Appl. Chemistry* 51, 709–729.

Pfennig N. 1977: Phototrophic green and purple bacteria: a comparative, systematic survey. *Ann. Rev. Microbiology* 31, 275–290.

Popov S.V. & Stolyarov A.S. 1996: Paleogeography and anoxic environemnts of the Oligocene-Early Miocene Paratethys. *Israel J. Earth Sci.* 45, 161–167.

Popov S.V., Akhmet'ev M.A., Zaporozhets N.I., Voronina A.A. & Stolyarov A.S. 1993: Evolution of Eastern Paratethys in the late Eocene-early Miocene. *Stratigraphy and Geological Correlation* 1, 6, 10–39.

Radke M., Willsch H. & Welte D.H. 1980: Preparative hydrocarbon group type determination by automated medium pressure liquid chromatography. *Analytical Chemistry* 52, 406–411.

Repeta D.J. 1993: A high resolution historical record of Holocene anoxygenic primary production in the Black Sea. *Geochim. Cosmochim. Acta* 57, 4337–4342.

Ricken W. 1991: Variation of sedimentation rates in rhythmically bedded sediments. Distinction between depositional types. In: Einsele G., Ricken W. & Seilacher A. (Eds.): Cycles and events in stratigraphy. *Springer,* Berlin, 167–187.

Rögl F. 1996: Stratigraphic correlation of the Paratethys Oligocene and Miocene. *Mitt. Gesell. Geol.-u. Bergbaustud. Österreich* 41, 65–73.

Rögl F. 1999: Mediterranean and Paratethys. Facts and hypotheses of an Oligocene to Miocene paleogeography (Short Overview). *Geol. Carpathica* 50, 4, 339–349.

Rögl F., Krhovský J., Braunstein R., Hamršmíd B., Sauer R. & Seifert P. 2001: The Ottenthal Formation revised — sedimentology, micropaleontology and stratigraphic correlation of the

Oligocene Ottenthal sections (Waschberg Unit, Lower Austria). In: Piller W.E. & Rasser M.W. (Eds.): Paleogene of the Eastern Alps. Österreichische Akademie der Wissenschaften. *Schriftenreihe der Erdwissenschaftlichen Kommissionen* 14, 291–346.

Rögl F., Krhovský J. & Hamršmíd B. 1997: Neue Beiträge zum Oligozän von Ottenthal in der Waschbergzone, Niederösterreich. *Österr. Geol. Gessel., Exkursionsführer* 17, 83–96.

Rusu A., Popescu G. & Melinte M. 1996: Field Symposium Oligocene — Miocene transition and main geological events in Romania, 28. August–2. September 1996. A. Excursion guide. *Inst. Geol. Romaniei, IGCP Project No. 326*, 1–47, 21 figs.

Sachs J.P. & Repeta D.J. 1999: Oligotrophy and nitrogen fixation during eastern Mediterranean sapropel events. *Science* 286, 2485–2488.

Schmidt F. & Erdogan L.T. 1996: Palaeohydrodynamics in exploration. In: Wessely G. & Liebl W. (Eds.): Oil and gas in Alpidic thrustbelts and basins of Central and Eastern Europe. *EAGE Special Publication 5. The Alden Press,* Oxford, 255–265.

Schmiedl G., Scherbacher M., Bruch A.A., Jelen B., Nebelsick J.H., Hemleben C., Mosbrugger V. & Rifelj H. 2002: Paleoenvironmental evolution of the Paratethys in the Slovenian Basin during the Late Paleogene. *Int. J. Earth Sci.* 91, 123–132.

Schulz H.-M., Sachsenhofer R.F., Bechtel A., Polesny H. & Wagner L. 2002: Origin of hydrocarbon source rocks in the Austrian Molasse Basin (Eocene–Oligocene transition). *Mar. Petroleum Geol.* 19, 6, 683–709.

Schwark L. & Püttmann W. 1990: Aromatic hydrocarbon composition of the Permian Kupferschiefer in the Lower Rhine Basin, N.W. Germany. *Organic Geochemistry* 16, 749–761.

Schwark L., Vliex M. & Schaeffer P. 1998: Geochemical characterization of Malm Zeta laminated carbonates from the Franconian Alb, SW-Germany (II). *Organic Geochemistry* 29, 8, 1921–1952.

Sinninghe Damsté J.S., Kock-Van Dalen A.C., De Leeuw J.W., Schenk P.A., Guo-ying S. & Brassell S.C. 1987a: The identification of mono-, di-, and trimethyl 2-methyl-2-(4,8,12-trimethyltridecyl) chromans and their occurrence in geosphere. *Geochim. Cosmochim. Acta* 51, 2393–2400.

Sinninghe Damsté J.S., Wakeham S.G., Kohnen M.E.L., Hayes J.M. & De Leeuw J.W. 1987b: A 6,000-year sedimentary molecular record of chemocline excursions in the Black Sea. *Nature* 362, 827–829.

Summons R.E. 1993: Biogeochemical cycles: A review of fundamental aspects of organic matter formation, preservation, and composition. In: Engel M.H. & Macko S.A. (Eds.): Organic geochemistry — principles and applications. *Plenum Press,* New York, 3–21.

Summons R.E. & Powell T.G. 1987: Identification of aryl isoprenoids in source rocks and crude oils: biological markers for the green sulphur bacteria. *Geochim. Cosmochim. Acta* 51, 557–566.

Tissot B.T. & Welte D.H. 1984: Petroleum formation and occurrences. 2. Ed. *Springer*, Berlin, 1–699.

Volkman J.K. 1986: A review of sterol markers for marine and terrigenous organic matter. *Organic Geochemistry* 9, 83–99.

Volkman J.K. & Maxwell J.R. 1986: Acyclic isoprenoids as biological markers. In: Johns R.B. (Ed.): Biological markers in the sedimentary record. *Elsevier*, Amsterdam, 1–42.

Voß M. & Struck U. 1997: Stable nitrogen and carbon isotopes as indicators of eutrophication of the Oder river (Baltic sea). *Mar. Chemistry* 59, 35–49.

Wagner L.R. 1996: Stratigraphy and hydrocarbons in Upper Austrian Molasse Foredeep (active margin). In: Wessely G. & Liebl W. (Eds.): Oil and gas in Alpidic thrustbelts and basins of Central and Eastern Europe. *EAGE Spec. Publ.* 5, 217–235.

Wagner L.R. 1998: Tectonostratigraphy and hydrocarbons in the Molasse Foredeep of Salzburg, Upper and Lower Austria. In: Mascle A., Puigdefàbregas C. & Luterbacher H.P. (Eds.): Cenozoic foreland basins of Western Europe. *Geol. Soc. Spec. Publ.* 134, 339–369.

Wagner L. & Wessely G. 1997: Exploration opportunities. In: Federal Ministry for Economic Affairs & Geological Survey of Austria (Ed.): Hydrocarbon potential and exploration opportunities in Austria. *Malek,* Krems, 19–33.

Wagner L., Kuckelkorn K. & Hiltmann W. 1986: Neue Ergebnisse zur alpinen Gebirgsbildung Oberösterreichs aus der Bohrung Oberhofen 1 — Stratigraphie, Fazies, Maturität und Tektonik. *Erdöl Erdgas Kohle* 102, 1, 12–19 (in German).

Wehner H. & Kuckelkorn K. 1995: Zur Herkunft der Erdöle im nördlichen Alpen-/Karpatenvorland. *Erdöl Erdgas Kohle* 111, 12, 508–514 (in German).

Wilkin R.T., Barnes H.L. & Brantley S.L. 1996: The size distribution of framboidal pyrite in modern sediments: An indicator of redox conditions. *Geochim. Cosmochim. Acta* 60, 3897–3912.

Ziegler P.A. 1987: Late Cretaceous and Cenozoic intraplate compressional deformations in the Alpine foreland — a geodynamic model. *Tectonophysics* 137, 389–420.

Ziegler P.A. & Roure F. 1999: Petroleum systems of Alpine-Mediterranean foldbelts and basins. In: Durand B., Loivet L., Horváth F. & Séranne M. (Eds.): The Mediteranean Basins: Tertiary extension within the Alpine Orogen. *Geol. Soc. London, Spec. Publ*. 156, 517–540.